

hep-th/0306099
CERN-TH/2003-126

No UV/IR Mixing in Unitary Space-Time Non-Commutative Field Theory

P. Fischer¹, V. Putz²

¹*Theory Division, CERN, CH-1211 Geneva 23, Switzerland*

²*Max-Planck-Institut für Mathematik in den Naturwissenschaften,
Inselstraße 22-26, D-04103 Leipzig, Germany*

Abstract

In this article we calculate several divergent amplitudes in ϕ^4 -theory on non-commutative space-time ($\Theta_{0i} \neq 0$) in the framework of Interaction-Point Time-Ordered Perturbation Theory (IPTOPT), continuing work done in hep-th/0209253. On the ground of these results we find corresponding Feynman rules that allow for a much easier diagrammatic calculation of amplitudes. The most important feature of the present theory is the absence of the UV/IR mixing problem in all amplitudes calculated so far. Although we are not yet able to give a rigorous proof, we provide a strong argument for this result to hold in general. Together with the Feynman rules we found, this opens promising vistas onto the systematic renormalization of non-commutative field theories.

¹pfischer@mail.cern.ch

²putz@hep.itp.tuwien.ac.at, work supported by the “Fonds zur Förderung der Wissenschaften” (FWF) under contract P15015-TPH.

1 Introduction

In quantum field theories on non-commutative spaces, we know of two major problems. The first one is the famous so-called “UV/IR mixing”. In using standard perturbative techniques a completely new type of non-renormalizable, infrared-like singularities occurs [1], [2]. Attempts to cure this imponderability have been made, but no convincing solution has been found so far.

The second problem is the loss of unitarity on non-commutative spaces with Minkowskian signature [3], [4]. The first resolutions made considerable, undesirable restrictions (e.g. commutativity of time) and were thus not very satisfying. In [5] and [6] two proposals to cure this severe problem have been made. A similar approach was elaborated in [7], [8]. There the Gell-Mann–Low formula for Green’s functions:

$$G_n(x_1, \dots, x_k) := \frac{i^n}{n!} \int d^4 z_1 \dots d^4 z_n \langle 0 | T\phi(x_1) \dots \phi(x_k) \mathcal{L}_I(z_1) \dots \mathcal{L}_I(z_n) | 0 \rangle^{con},$$

was used. The theory is quantized canonically in Minkowski space instead of employing the Euclidean path-integral (PI). As shown in [3], [6] and [8], unitarity is recovered by choosing the Lagrangian as the starting point of this formulation of non-commutative field theories. It must be stressed that for non-commutative time ($\Theta_{0i} \neq 0$) a theory different from the usual approach is considered and new results are to be expected.

Technically this can easily be seen by noting that time ordering (TO) – which contains $\Theta(x^0 - y^0)$ – stands *in front* of the \star -product, which, in the formulation $f(x) \star g(x) := e^{i/2\partial_{x,\mu}\Theta^{\mu\nu}\partial_{y,\nu}} f(x)g(y)|_{x=y}$, contains an infinite number of time derivations for $\Theta_{0i} \neq 0$. The consequences of this rather obvious fact were investigated in detail in [7], [8] for ϕ^3 and ϕ^4 in [9] for ϕ^4 .

In this last work it was also shown that if one employs another definition of the \star -product,

$$\begin{aligned} \mathcal{L}_I(z_l) &= \frac{g}{4!} (\phi \star \phi \star \phi \star \phi)(z_l) = \int \prod_{i=1}^3 \left(d^4 s_i \frac{d^4 l_i}{(2\pi)^4} e^{il_i s_i} \right) \\ &\quad \times \phi(z_l - \frac{\tilde{l}_1}{2}) \phi(z_l + s_1 - \frac{\tilde{l}_2}{2}) \phi(z_l + s_1 + s_2 - \frac{\tilde{l}_3}{2}) \phi(z_l + s_1 + s_2 + s_3), \end{aligned} \quad (1)$$

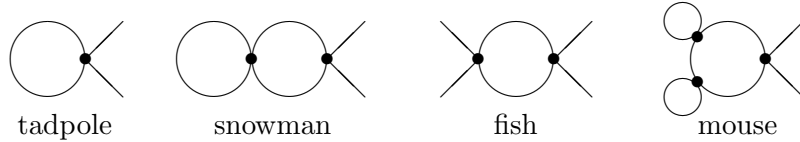
a physical interpretation of the ensuing techniques is possible (aside from making the calculations easier and more transparent). Non-commutativity can be seen explicitly to “spread” the interaction over space-time. The time ordering only acts on the time-stamp of the interaction point (IP) z_l^0 , but not on the new, smeared-out “physical” coordinates of the field operators. Thus the four fields of the interaction point are not time-ordered with respect to each other, time ordering being realized between external and interaction points only. This fact gave reason to the notion of *Interaction-Point Time-Ordered Perturbation Theory* (IPTOPT) introduced in [9], to distinguish

from a true causal time ordering. The fields at the interaction point are not causally connected, and “micro-” (better “nano-”) causality is violated at the non-commutative vertex [9], [10].

In [9] this approach was developed into IPTOPT in analogy to pre-Feynmanian commutative perturbation theory [11]. The techniques developed so far are still rather cumbersome (though examples of their applicability are given below) and true diagrammatics including the respective Feynman rules (FR) are the next step in the implementation of this program.

This is undertaken in the present work (see also [12]), which already rewards us with a possible solution to the second great problem of non-commutative field theories, UV/IR mixing.

To reach these goals we set out from previous work. In section 2 we employ the non-commutative version of the time ordered expression for Green functions [11], eq. (39) of [9], to obtain explicit results for the Fourier-transformed (FT), amputated on-shell two-point one-loop amplitude $\Gamma^{(2,1)}$ (tadpole, fig. 1), two-point two-loop amplitude $\Gamma^{(2,2)}$ (snowman, fig. 2), and four-point one-loop amplitude $\Gamma^{(4,1)}$ (fish, fig. 3).



In section 3 we return to the result for the off-shell non-amputated Green function $G^{(2,1)}$ obtained in [9] by explicitly commuting out the free field operators. Retracing one step, we explicitly state the full off-shell amplitude, the correction to the propagator at one loop.

This result allows us to “read off” the TO propagator of our theory and the algorithm that allows us the construction of general diagrams.

The last missing item, the vertex, is easily obtained and completes the set of FR of IPTOPT.

Section 4 is devoted to a demonstration of the correctness and applicability of our new FR by employing them in redoing the calculations of section 2. Of special interest to the issue of UV/IR mixing is a certain two-point three-loop amplitude $\Gamma^{(2,3)}$ (two tadpoles inserted into a third, the so-called *mouse*-diagram of fig. 4), where it generates new divergences. We calculate this expression in section 4.4.

The discussion of section 5 is mainly dedicated to what our results tell us about the UV/IR problem. First we note that it does not appear anywhere in the determined amplitudes, especially not in $\Gamma^{(2,3)}$ which remains – in contrast to the results normally obtained in non-commutative field theory – void of new divergences. This most interesting feature of the present theory encourages us to put forth a general argument for the absence of this

notorious problem in IPTOPT, which we do in section 5.2, at least in its usual form. A short remark on the PT invariance of the obtained amplitudes is made in section 5.3.

In the Outlook, section 6, we give lines along which a rigorous proof (or disclaim) of the general absence of UV/IR mixing in IPTOPT may proceed. We also list the next steps in the program of IPTOPT, among which are of course the attempt at a renormalization of this non-commutative field theory.

2 Examples

Now we want to look at some prominent diagrams with the help of eq. (39) of [9]:

$$\begin{aligned}
& \Gamma(q_1^{\sigma_1}, \dots, q_E^{\sigma_E}) \\
&= \lim_{\varepsilon \rightarrow 0} \frac{g^V}{(4!)^V} \int \prod_{i=1}^I \frac{d^3 k_i}{(2\pi)^3 2\omega_{k_i}} \prod_{v=1}^{V-1} \frac{i(2\pi)^3 \delta^3 \left(\sum_{i=1}^I J_{vi} \vec{k}_i + \sum_{e=1}^E J_{ve} \sigma_e \vec{q}_e \right)}{\sum_{v' \leq v} \left(\sum_{i=1}^I J_{v'i} \omega_{k_i} + \sum_{e=1}^E J_{v'e} \omega_{q_e} \right) + i\varepsilon} \\
& \times \exp \left(i\theta^{\mu\nu} \left(\sum_{i,j=1}^I I_{ij} k_{i,\mu}^+ k_{j,\nu}^+ + \sum_{i=1}^I \sum_{e=1}^E I_{ie} \sigma_e k_{i,\mu}^+ q_{e,\nu}^{\sigma_e} + \sum_{e,f=1}^E I_{ef} \sigma_e \sigma_f q_{e,\mu}^{\sigma_e} q_{f,\nu}^{\sigma_f} \right) \right). \tag{2}
\end{aligned}$$

The vertex that is missing in the product over v is the latest one. Note that this formula, because of the somewhat unusual definition of the S-matrix used in [9], has some extra factors i with respect to the usual expression.

Here the internal (carrying the momenta k) and external (carrying the momenta q) lines are oriented forward in time (note, however, that the external *momenta* are always defined outgoing of a vertex). Then, the incidence matrices J_{vi}, J_{ve} are equal to -1 if the line leaves v and to $+1$ if the line arrives at v . Similarly, $\sigma_e = -1$ if the line e leaves x_e and $\sigma_e = +1$ if the line e arrives at x_e . The matrices I_{ij}, I_{ie}, I_{ef} are the intersection matrices, which describe the time configuration of the lines at a vertex. They will be defined below.

2.1 Two-Point One-Loop Tadpole

To see how the formula works, we first want to review the on-shell one-loop correction to the two-point function. One typical contribution to this diagram is: With eq. (2) a general contribution reads

$$\Gamma^{(2,1)} = \frac{g}{4!} \int \frac{d^3 k}{(2\pi)^3 2\omega_k} \cdot 1 \cdot \exp(i\theta^{\mu\nu} \phi_{\mu\nu}), \tag{3}$$

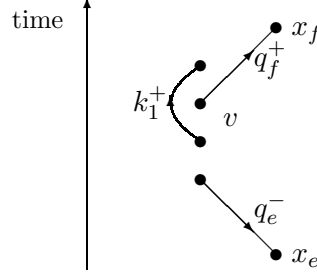


Figure 1: The contribution $(e, \bar{1}, f, 1)$

where $\Phi_{\mu\nu}$ is the phase depending on the special configuration of lines at the vertex. Since there is only one inner line, the I_{ij} term in (2) is vanishing. For the I_{ie} term we have to look at all possible configurations of lines at the 4-field vertex v . We have

$$I_{ij} = \frac{1}{2} \sum_v \tau_{ij}^v J_{vi} J_{vj}, \quad I_{ie} = \frac{1}{2} \sum_v (\tau_{ie}^v - \tau_{ei}^v) J_{vi} J_{ve}, \quad I_{ef} = \frac{1}{2} \sum_v \tau_{ef}^v J_{ve} J_{vf}. \quad (4)$$

The sum is over all vertices in a particular graph; $\tau_{ie}^v = +1$ if the line i is connected to an “earlier” field ϕ in the vertex v than the line e , otherwise $\tau_{ij}^v = 0$. We have $\sigma_e = -1$, $J_{ve} = +1$, $\sigma_f = +1$, $J_{vf} = -1$. For the inner line we have to distinguish between the one leaving (we denote this by $i = \bar{1}$) and the one arriving ($i = 1$). Then $J_{v\bar{1}} = -1$ and $J_{v1} = +1$. Note that the inner line is by definition oriented forward in time and $k_1 \equiv k_{\bar{1}}$. We write the time-ordering configuration at the vertex as an array, the contribution in figure 1 is labelled $(e, \bar{1}, f, 1)$. Then we find, for the I_{ie} and the I_{ef} terms:

$$\begin{aligned} \sum_{i=1, \bar{1}} k_i^+ I_{ie}(-q_e^-) + \sum_{i=1, \bar{1}} k_i^+ I_{if}(+q_f^+) + \sum_{e', f' = e, f} I_{e' f'}(\sigma_{e'} q_{e'}^{\sigma_{e'}})(\sigma_{f'} q_{f'}^{\sigma_{f'}}) = \\ (e, f, \bar{1}, 1) : 0 + 0 + \frac{1}{2} q_e^- q_f^+ &\quad (f, e, \bar{1}, 1) : 0 + 0 + \frac{1}{2} q_f^+ q_e^- \\ (\bar{1}, 1, e, f) : 0 + 0 + \frac{1}{2} q_e^- q_f^+ &\quad (\bar{1}, 1, f, e) : 0 + 0 + \frac{1}{2} q_f^+ q_e^- \\ (e, \bar{1}, 1, f) : 0 + 0 + \frac{1}{2} q_e^- q_f^+ &\quad (f, \bar{1}, 1, e) : 0 + 0 + \frac{1}{2} q_f^+ q_e^- \\ (\bar{1}, e, f, 1) : -k_1^+(-q_e^-) + k_1^+ q_f^+ + \frac{1}{2} q_e^- q_f^+ &\quad (\bar{1}, f, e, 1) : -k_1^+(-q_e^-) + k_1^+ q_f^+ + \frac{1}{2} q_f^+ q_e^- \\ (e, \bar{1}, f, 1) : +k_1^+ q_f^+ + \frac{1}{2} q_e^- q_f^+ &\quad (\bar{1}, f, 1, e) : +k_1^+ q_f^+ + \frac{1}{2} q_f^+ q_e^- \\ (\bar{1}, e, 1, f) : -k_1^+(-q_e^-) + \frac{1}{2} q_e^- q_f^+ &\quad (f, \bar{1}, e, 1) : -k_1^+(-q_e^-) + \frac{1}{2} q_f^+ q_e^- \end{aligned}$$

Thus for the sum over all possible phase factors, we obtain

$$\sum_{\phi} \exp(i\theta^{\mu\nu}\phi_{\mu\nu}) = 2 \cos\left(\frac{1}{2}\theta^{\mu\nu}q_{e,\mu}^-q_{f,\nu}^+\right) \times \left(3e^0 + e^{i\theta^{\mu\nu}k_{1,\mu}^+q_{e,\nu}^-} + e^{i\theta^{\mu\nu}k_{1,\mu}^+q_{f,\nu}^+} + e^{i\theta^{\mu\nu}(k_{1,\mu}^+q_{e,\nu}^- + k_{1,\mu}^+q_{f,\nu}^+)}\right). \quad (5)$$

Inserting this into (3) and with $q_f^+ = -q_e^-$ we find for the total Γ

$$\Gamma_{tot}^{(2,1)} = \frac{g}{12} \int \frac{d^3k}{(2\pi)^3 2\omega_k} (4 + 2 \cos(\theta^{\mu\nu}k_{\mu}^+q_{\nu}^+)). \quad (6)$$

This result agrees with eq. (25) of [9], where the same amplitude was obtained by explicitly commuting out the free field operators.

2.2 Two-Loop Snowman

For the two-loop snowman, in addition to the inner configuration of the lines at the vertices, we have to respect the two possibilities of time ordering of the vertices:

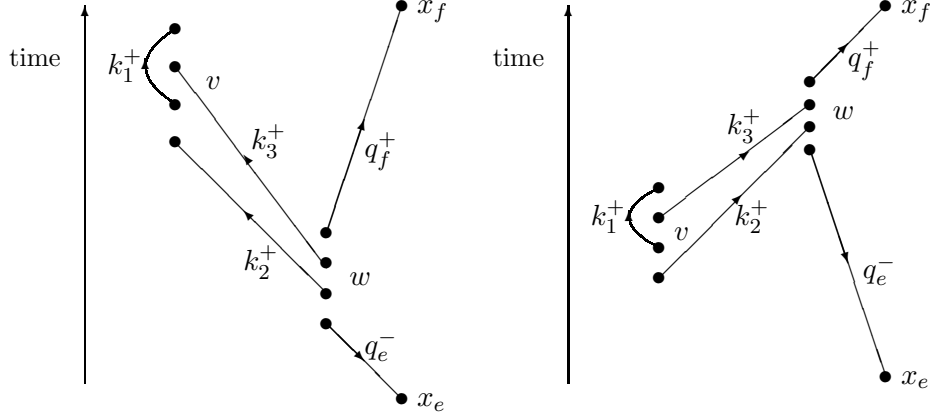


Figure 2: $(2, \bar{1}, 3, 1) \times (e, \bar{2}, \bar{3}, f)$ $(e, \bar{2}, \bar{3}, f) \times (2, \bar{1}, 3, 1)$

With $V = 2$, $E = 2$, $I = 3$, eq. (2) reads for the left graph, where the vertex v is before the vertex w :

$$\Gamma^{(2,2)} = \frac{g^2}{(4!)^2} \int \frac{d^3k_1 d^3k_2 d^3k_3}{(2\pi)^9 8\omega_1 \omega_2 \omega_3} \frac{i(2\pi)^3 \delta^3(-\vec{k}_2 - \vec{k}_3 - \vec{q}_e - \vec{q}_f)}{-\omega_2 - \omega_3 + \omega_e - \omega_f + i\varepsilon} \exp(i\theta^{\mu\nu}\phi_{\mu\nu}). \quad (7)$$

We have $J_{v2} = J_{v3} = +1$, $J_{w2} = J_{w3} = -1$, $\sigma_e = +1$, $\sigma_f = -1$. We obtain a non-trivial I_{ij} term from the vertex v . For example, the phase of the vertex

v in the left graph is

$$(2, \bar{1}, 3, 1)_v : -k_1^+ k_3^+ + \frac{1}{2} k_2^+ k_3^+, \quad (8)$$

and is similar for the other 11 contributions. For the vertex w the I_{ij} and I_{ie} terms are non-zero. Again, we present only one contribution (note that $-q_e^- = +q_f^+$, owing to momentum conservation):

$$\begin{aligned} (e, 2, 3, f)_w : \quad & \frac{1}{2} k_2^+ (-q_e^-) + \frac{1}{2} k_3^+ (-q_e^-) + \frac{1}{2} k_2^+ q_f^+ + \frac{1}{2} k_3^+ q_f^+ + \frac{1}{2} k_2^+ k_3^+ \\ & = k_2^+ q_f^+ + k_3^+ q_f^+ + \frac{1}{2} k_2^+ k_3^+. \end{aligned} \quad (9)$$

Collecting the other 23 terms would be fairly edifying for a computer. Summing up all contributions, using again $q_e^- = -q_f^+$, integrating out \vec{k}_3 and setting $\varepsilon = 0$ yields

$$\begin{aligned} \Gamma_{left}^{(2,2)} = & -\frac{ig^2}{(4!)^2} \int \frac{d^3 k_2}{(2\pi)^3 8\omega_2^3} \int \frac{d^3 k_1}{(2\pi)^3 2\omega_1} 2 \cos\left(\frac{1}{2} k_2^+ \tilde{k}_2^-\right) \\ & \times \left(3 + e^{-i\theta^{\mu\nu} k_{1,\mu}^+ k_{2,\nu}^+} + e^{+i\theta^{\mu\nu} k_{1,\mu}^+ k_{2,\nu}^-} + e^{-i\theta^{\mu\nu} (k_{1,\mu}^+ k_{2,\nu}^+ - k_{1,\mu}^- k_{2,\nu}^-)} \right) \\ & \times 2 \cos\left(\frac{1}{2} k_2^+ \tilde{k}_2^-\right) \left(6 + 2 \cos(\theta^{\mu\nu} k_{2,\mu}^+ q_{f,\nu}^+) \right. \\ & \left. + 2 \cos(\theta^{\mu\nu} k_{2,\mu}^- q_{f,\nu}^+) + 2 \cos(\theta^{\mu\nu} (k_{2,\mu}^+ - k_{2,\mu}^-) q_{f,\nu}^+) \right). \end{aligned} \quad (10)$$

The first two lines of the integral kernel are exactly eq. (6), with the obvious replacements (note the correct signs coming from the σ 's and J 's) $-q_e^- \rightarrow +k_2^+$ and $-q_f^+ \rightarrow +k_3^+ \rightarrow -k_2^-$. For $\Gamma_{right}^{(2,2)}$ we find the same expression with $k_{2,3}^+ \rightarrow -k_{2,3}^+$, because of the reversed sign of J_{ve} , etc. This yields exactly the complex-conjugated expression, so with the help of $4 \cos^2(\frac{x}{2}) = 2 + 2 \cos(x)$ we get

$$\begin{aligned} \Gamma_{tot}^{(2,2)} = & -\frac{ig^2}{(4!)^2} \int \frac{d^3 k_2}{(2\pi)^3 8\omega_2^3} (2 + 2 \cos(k_2^+ \tilde{k}_2^-)) \\ & \times \left(6 + 2 \cos(k_2^+ \tilde{q}_f^+) + 2 \cos(k_2^- \tilde{q}_f^+) + 2 \cos((k_2^+ - k_2^-) \tilde{q}_f^+) \right) \\ & \times \int \frac{d^3 k_1}{(2\pi)^3 2\omega_1} \left(6 + 2 \cos(k_1^+ \tilde{k}_2^+) + 2 \cos(k_1^- \tilde{k}_2^-) + 2 \cos(k_1^+ (\tilde{k}_2^+ - \tilde{k}_2^-)) \right). \end{aligned} \quad (11)$$

Note the extra i due to the slightly unusual definition of the S-matrix used in [9].

2.3 Four-Point One-Loop Correction

Finally, for the one-loop correction to the t -channel four-point function we have the contributions of figure 3.

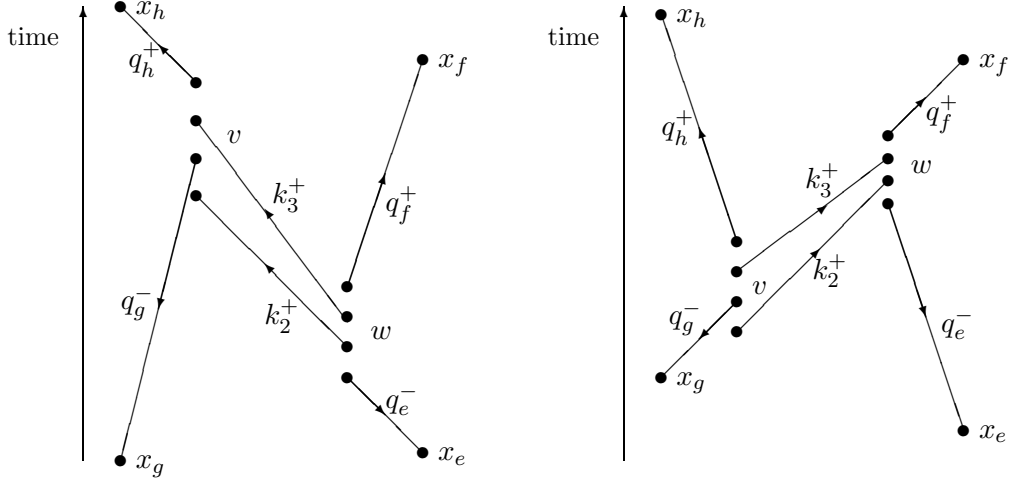


Figure 3: Two contributions to $\Gamma^{(4,1)}$

Without going into detail with respect to the phase, we can prove the IR finiteness of the sum of these contributions:

$$\begin{aligned}
 \Gamma^{(4,1)} &= \frac{g^2}{(4!)^2} \int \frac{d^3 k_2}{(2\pi)^3 2\omega_2} \int \frac{d^3 k_3}{(2\pi)^3 2\omega_3} \\
 &\times \left(\frac{i(2\pi)^3 \delta^3(-\vec{k}_2 - \vec{k}_3 - \vec{q}_e - \vec{q}_f)}{-\omega_2 - \omega_3 + \omega_e - \omega_f + i\varepsilon} \right. \\
 &\times \Psi(-q_e^-, -q_f^+, -k_2^+, -k_3^+) \Psi(-q_g^-, -q_h^+, k_2^+, k_3^+) \\
 &+ \frac{i(2\pi)^3 \delta^3(-\vec{k}_2 - \vec{k}_3 - \vec{q}_g - \vec{q}_h)}{-\omega_2 - \omega_3 + \omega_g - \omega_h + i\varepsilon} \\
 &\left. \times \Psi(-q_e^-, -q_f^+, +k_2^+, +k_3^+) \Psi(-q_g^-, -q_h^+, -k_2^+, -k_3^+) \right). \tag{12}
 \end{aligned}$$

Here the phase Ψ will be defined in section 3.5. With conservation of the global 4-momentum $\delta^4(q_e^- + q_f^+ + q_g^- + q_h^+)$, we have $\omega_g - \omega_h = -(\omega_e - \omega_f)$ in the denominator of the second term. Before integrating out k_3 we let $\vec{k}_2 \rightarrow -\vec{k}_2$, $\vec{k}_3 \rightarrow -\vec{k}_3$ in the second term, so that $\vec{k}_3 = -\vec{k}_2 - \vec{q}_e - \vec{q}_f$ in both terms. Thus we find

$$\begin{aligned}
 \Gamma^{(4,1)} &= -\frac{g^2}{(4!)^2} \int \frac{d^3 k_2}{(2\pi)^3 2\omega_2} \frac{1}{(2\pi)^3 2\omega_3} i(2\pi)^3 \\
 &\times \left(\frac{\Psi(-q_e^-, -q_f^+, -k_2^+, -k_3^+) \Psi(-q_g^-, -q_h^+, k_2^+, k_3^+)}{\omega_2 + \omega_3 - (\omega_e - \omega_f) - i\varepsilon} \right. \\
 &+ \left. \frac{\Psi(-q_e^-, -q_f^+, -k_2^-, -k_3^-) \Psi(-q_g^-, -q_h^+, k_2^-, k_3^-)}{\omega_2 + \omega_3 + (\omega_e - \omega_f) - i\varepsilon} \right) \Big|_{\vec{k}_3 = -(\vec{k}_2 + \vec{q}_e + \vec{q}_f)}. \tag{13}
 \end{aligned}$$

We find that the denominators are strictly positive,

$$\begin{aligned}
& |(\omega_2 + \omega_3)|^2 - |(\omega_e - \omega_f)|^2 = \\
& \vec{k}_2^2 + m^2 + (\vec{k}_2 + \vec{q}_e + \vec{q}_f)^2 + m^2 + 2\omega_2\omega_3 \\
& - \vec{q}_e^2 - m^2 - \vec{q}_f^2 - m^2 + 2\omega_e\omega_f = \\
& 2\left(\vec{k}_2(\vec{k}_2 + \vec{q}_e + \vec{q}_f) + \vec{q}_e\vec{q}_f + \omega_2\omega_3 + \omega_e\omega_f\right) \Big|_{\vec{k}_3 = -(\vec{k}_2 + \vec{q}_e + \vec{q}_f)} > 0 \\
& (|\vec{p} \cdot \vec{q}| < \omega_p\omega_q, m > 0).
\end{aligned}$$

Thus, no new kinematic IR divergence occurs with respect to the commutative case, although the usual cancellations could not take place because of the different phases. Hence we made sure that no novel problems arise from this quarter.

3 The Feynman Rules for IPTOPT

To obtain the set of diagrammatic rules for our model we have to answer three questions:

1. What is the vertex?
2. What is the propagator?
3. How to construct graphs?

The first of these we postpone to section 3.5, while the other two are tackled by retracing our steps to the explicit result for the tadpole obtained in [9].

3.1 The Full Non-Commutative Propagator

We start our search for the Feynman(-like) rules of non-commutative IPTOPT at the explicit expression for the two-point one-loop tadpole $G^{(2,1)}$, eq. (24) of [9].

Repeating the notation from [9] (recall that $p^\pm := (\pm\omega_p, \vec{p})$, $\omega_p := \sqrt{\vec{p}^2 + m^2}$, $\tilde{p}^\nu := p_\mu \theta^{\mu\nu}$):

$$\begin{aligned}
\mathcal{I}^{\pm\pm}((\pm p)^+, (\pm q)^+) &= \int \frac{d^3 k}{(2\pi)^3 2\omega_k} (3 + e^{ip^\pm \tilde{k}^+ + iq^\pm \tilde{k}^+} + e^{ip^\pm \tilde{k}^+} + e^{iq^\pm \tilde{k}^+}) \\
&\equiv \mathcal{I}(p^\pm, q^\pm),
\end{aligned} \tag{14}$$

we retrace one step and give the unamputated FT Green function

$$\begin{aligned}
G^{(2,1)}(p, q) = & -\lim_{\delta_1, \delta_2 \rightarrow 0} \frac{g}{12} (2\pi)^4 \delta(p + q) \\
& \times \left(\frac{1}{p_0 - \omega_p + i\delta_1} \frac{1}{\omega_p + \omega_q - i\delta_2} \frac{\cos(\frac{1}{2}p^+ \tilde{q}^+)}{4\omega_p \omega_q} \mathcal{I}(p^+, q^+) \right. \\
& + \frac{1}{q_0 - \omega_q + i\delta_1} \frac{1}{\omega_p + \omega_q - i\delta_2} \frac{\cos(\frac{1}{2}p^+ \tilde{q}^+)}{4\omega_p \omega_q} \mathcal{I}(p^+, q^+) \\
& + \frac{1}{p_0 - \omega_p + i\delta_1} \frac{1}{q_0 + \omega_q - i\delta_2} \frac{\cos(\frac{1}{2}p^+ \tilde{q}^-)}{4\omega_p \omega_q} \mathcal{I}(p^+, q^-) \\
& + \frac{1}{q_0 - \omega_q + i\delta_1} \frac{1}{p_0 + \omega_p - i\delta_2} \frac{\cos(\frac{1}{2}p^- \tilde{q}^+)}{4\omega_p \omega_q} \mathcal{I}(p^-, q^+) \\
& + \frac{1}{\omega_p + \omega_q - i\delta_1} \frac{1}{-q_0 - \omega_q + i\delta_2} \frac{\cos(\frac{1}{2}p^- \tilde{q}^-)}{4\omega_p \omega_q} \mathcal{I}(p^-, q^-) \\
& \left. + \frac{1}{\omega_p + \omega_q - i\delta_1} \frac{1}{-p_0 - \omega_p + i\delta_2} \frac{\cos(\frac{1}{2}p^- \tilde{q}^-)}{4\omega_p \omega_q} \mathcal{I}(p^-, q^-) \right). \quad (15)
\end{aligned}$$

Making use of local energy-momentum conservation $p^0 = -q^0$ and $\omega_p = +\omega_q$, and of the relation $q^\pm = -p^\mp$, we eliminate q and contract eq. (15) to

$$\begin{aligned}
G^{(2,1)}(p) = & -\lim_{\varepsilon \rightarrow 0} \frac{g}{12(2\omega_p)^2} (2\pi)^4 \delta(p + q) \\
& \times \left(\frac{1}{p_0 - \omega_p + i\varepsilon} \frac{1}{p_0 + \omega_p - i\varepsilon} \cos\left(\frac{1}{2}p^+ \tilde{p}^-\right) (\mathcal{I}(p^+, -p^-) + \mathcal{I}(p^-, -p^+)) \right. \\
& - \frac{1}{p_0 - \omega_p + i\varepsilon} \frac{1}{p_0 - \omega_p + i\varepsilon} \cos\left(\frac{1}{2}p^+ \tilde{p}^+\right) \mathcal{I}(p^+, -p^+) \\
& \left. - \frac{1}{p_0 + \omega_p - i\varepsilon} \frac{1}{p_0 + \omega_p - i\varepsilon} \cos\left(\frac{1}{2}p^- \tilde{p}^-\right) \mathcal{I}(p^-, -p^-) \right). \quad (16)
\end{aligned}$$

This can easily be written as the sum over two signs:

$$\begin{aligned}
G^{(2,1)}(p) = & \frac{g}{12} (2\pi)^4 \delta(p + q) \sum_{\sigma}^{+1, -1} \sum_{\sigma'}^{+1, -1} \cos(p^\sigma \tilde{p}^{\sigma'}) \mathcal{I}(p^\sigma, -p^{\sigma'}) \\
& \frac{1}{2\omega_p} \frac{1}{\sigma p_0 - \omega_p + i\varepsilon} \frac{1}{2\omega_p} \frac{1}{\sigma' p_0 - \omega_p + i\varepsilon}. \quad (17)
\end{aligned}$$

3.2 The TO Propagator

Equation (17) lets us read off the answers to both our questions. Since we have not performed any amputation yet, two propagators must be included in the above expression. We easily identify the TO propagator as

$$i\Delta^{TO} := \frac{\delta_{\sigma, -\sigma'}}{2\omega_p} \frac{i}{\sigma p^0 - \omega_p + i\varepsilon}. \quad (18)$$

The $\delta_{\sigma,-\sigma'}$ was included to guarantee TO-diagrammatic consistency: every directed TO line that leaves one vertex (σ) has to arrive at another one (σ'). (The correctness of this addition will become evident in the following examples.)

Note that the same result is independently obtained in [12], where the TO propagator is called “contractor”.

The global TO of the vertices is another necessary issue to be encoded in Δ^{TO} : every line has to leave its earlier vertex and arrive at its later vertex, and this must be consistently so for all lines of the diagram. This property is taken care of by the sign of the pole prescription. As illustrated in the amplitudes (re)calculated in section 4, only products of TO propagators in TO consistent graphs (if $A < B$ and $C < A$ then $C < B$) will contribute. All others (e.g. $A < B$ and $C < A$ but $B < C$) will have their poles bundled in the same complex half-plane and hence vanish upon integrating over p^0 .

3.3 Building Graphs

In addition to providing us with a propagator, eq. (17) also tells us how to construct graphs: multiply together all the building blocks for a graph of given topology — lines, vertices, subgraphs — which all depend on the entering or leaving ($\sigma_i = \pm 1$) of the lines running into them. Then sum over all signs. The propagators take care of the correct connection of all parts of the diagram, especially causal consistency: if vertex A is later than vertex B and B is later than C, than A is also later than C.

Even at this point we may already calculate the two-point zero-loop function, the usual covariant propagator,

$$\begin{aligned} i\Delta_F &= \sum_{\sigma}^{+1,-1} i\Delta^{TO}(\sigma) = \sum_{\sigma}^{+1,-1} \frac{1}{2\omega} \frac{i}{\sigma p_0 - \omega + i\varepsilon} \\ &= \frac{i}{2\omega} \left(\frac{1}{+p_0 - \omega + i\varepsilon} + \frac{1}{-p_0 - \omega + i\varepsilon} \right) = \frac{i}{p_0^2 - \omega^2 + i\varepsilon}. \end{aligned} \quad (19)$$

3.4 Complete One-Loop Integrals

To complete our discussion of $G^{(2,1)}$, and for further use in section 4.4, we evaluate the \mathcal{I} ’s occurring in eq. (17).

Abbreviating the (cut-off-regularized) divergent part of the planar term by $\mathcal{Q} = \Lambda^2 + \frac{m^2}{2} \ln(\frac{m^2}{\Lambda^2})$, we give $\mathcal{I}(p^+, -p^+)$, which was already calculated in [9], eq. (31):

$$\mathcal{I}(p^+, -p^+) = \frac{2}{(2\pi)^2} \left(\mathcal{Q} - \sqrt{-\frac{m^2}{\tilde{p}_+^2}} K_1 \left(\sqrt{-m^2 \tilde{p}_+^2} \right) \right). \quad (20)$$

Analogously we find

$$\mathcal{I}(p^-, -p^-) = \frac{2}{(2\pi)^2} \left(\mathcal{Q} - \sqrt{-\frac{m^2}{\tilde{p}_-^2}} K_1 \left(\sqrt{-m^2 \tilde{p}_-^2} \right) \right). \quad (21)$$

Calculating the sum of the remaining integrals still has to be done. Adding the integrands gives

$$\begin{aligned} \mathcal{I}(p^+, -p^-) + \mathcal{I}(p^-, -p^+) &= \\ &= \int \frac{d^3 k}{(2\pi)^3 2\omega_k} (6 + e^{-ik^+ \tilde{p}^+ + ik^+ \tilde{p}^-} + e^{-ik^+ \tilde{p}^+} + e^{+ik^+ \tilde{p}^-} \\ &\quad + e^{+ik^+ \tilde{p}^+ - ik^+ \tilde{p}^-} + e^{+ik^+ \tilde{p}^+} + e^{-ik^+ \tilde{p}^-}) \quad (22) \\ &= \int \frac{d^3 k}{(2\pi)^3 2\omega_k} 2(3 + \cos(k^+ \tilde{p}^+) + \cos(k^+ \tilde{p}^-) + \cos(k^+ (\tilde{p}^+ - \tilde{p}^-))). \end{aligned}$$

The first and second cosine terms are just the ones yielding the non-planar parts of eqs. (20) and (21). The third one has to be dealt with explicitly. With $(\tilde{p}^+ - \tilde{p}^-)_\mu = 2\Theta_{0\mu}\omega$ and $\theta_{00} = 0$ we can choose a coordinate system with the z -axis parallel to the 3-vector θ_{0i} . Thus integrating out the angles yields

$$\frac{2}{(2\pi)^2 |\Theta_{0i}| \omega} \int_0^\infty dk \frac{|\vec{k}|}{\omega_k} \sin(2|\vec{k}| |\Theta_{0i}| \omega). \quad (23)$$

This we evaluate as

$$= \frac{m}{(2\pi)^2 |\Theta_{0i}| \omega} K_1(2m |\Theta_{0i}| \omega). \quad (24)$$

Hence we have

$$\begin{aligned} \mathcal{I}(p^+, -p^-) + \mathcal{I}(p^-, -p^+) &= \frac{2}{(2\pi)^2} \left(\frac{3}{2} \mathcal{Q} - 2 \frac{m}{|\tilde{p}^+|} K_1(m |\tilde{p}^+|) \right. \\ &\quad \left. - 2 \frac{m}{|\tilde{p}^-|} K_1(m |\tilde{p}^-|) + \frac{m}{|\Theta_{0i}| \omega} K_1(2m |\Theta_{0i}| \omega) \right). \quad (25) \end{aligned}$$

For further use (eq. (41)), we finally present another result. Iff $\mathcal{I}(p^+, -p^-)$ occurs under an integral over $d^3 p$ together with functions $f(\vec{p})$ invariant under $\vec{p} \rightarrow -\vec{p}$ we have:

$$\begin{aligned} \int d^3 p f(\vec{p}) \mathcal{I}(p^+, -p^-) &= \int d^3 p f(\vec{p}) \frac{1}{(2\pi)^2} \\ &\times \left(\frac{3}{2} \mathcal{Q} - \frac{2m}{|\tilde{p}^+|} K_1(m |\tilde{p}^+|) - \frac{2m}{|\tilde{p}^-|} K_1(m |\tilde{p}^-|) + \frac{m}{\omega_p |\Theta_{0i}|} K_1(2m \omega_p |\Theta_{0i}|) \right). \quad (26) \end{aligned}$$

$\mathcal{I}(p^-, -p^+)$ yields an identical result under the same assumption.

3.5 The Vertex

To answer our first question we straightforwardly peruse eq. (2) for no internal lines and four external ones with general causalities (σ 's). Summing over all possible inner (nano-) TO of the vertex, we proceed as in section 2 and find ($\tilde{p}^\nu := p_\mu \theta^{\mu\nu}$)

$$\begin{aligned} \Gamma^{(4,0)}(p_1^{\sigma_1}, p_2^{\sigma_2}, p_3^{\sigma_3}, p_4^{\sigma_4}) &:= \frac{g}{4!} \Psi(-p_1^{\sigma_1}, -p_2^{\sigma_2}, -p_3^{\sigma_3}, -p_4^{\sigma_4}) = \\ &= \frac{g}{3} \left(\cos\left(\frac{1}{2} p_1^{\sigma_1} \tilde{p}_2^{\sigma_2}\right) \cos\left(\frac{1}{2} p_3^{\sigma_3} \tilde{p}_4^{\sigma_4}\right) \cos\left(\frac{1}{2} (p_1^{\sigma_1} + p_2^{\sigma_2})(\tilde{p}_3^{\sigma_3} + \tilde{p}_4^{\sigma_4})\right) \right. \\ &\quad \left. + (2) \leftrightarrow (3) + (2) \leftrightarrow (4) \right). \end{aligned} \quad (27)$$

Note that here all the momenta are defined outgoing of the vertex. With the symmetry of the cosine we explicitly check the invariance of (27) with respect to any permutation of the momenta.

Unfortunately, the tadpole has to be treated separately. From eq. (2) it follows that the tadpole line has to be oriented forward in time. Thus only $\frac{24!}{2}$ nano-configurations at the vertex contribute. We find for the phase factor of a 1-loop tadpole (defining $p_2^{\sigma_2}$, $p_3^{\sigma_3}$ outgoing, loop momentum p_1^+)

$$\begin{aligned} \frac{g}{4!} \exp\left(i\theta_{\mu\nu} \sum_{a,b=1}^3 \tau_{ab}^v p_a^{\sigma_a} p_b^{\sigma_b}\right) &=: \frac{g}{4!} \Phi(p_1^+; -p_2^{\sigma_2}, -p_3^{\sigma_3}) \\ &= \frac{g}{12} \left(3 + e^{ip_1^+ \tilde{p}_2^{\sigma_2}} + e^{ip_1^+ \tilde{p}_3^{\sigma_3}} + e^{ip_1^+ (\tilde{p}_2^{\sigma_2} + \tilde{p}_3^{\sigma_3})} \right) \cos\left(\frac{1}{2} p_2^{\sigma_2} \tilde{p}_3^{\sigma_3}\right). \end{aligned} \quad (28)$$

3.6 Summary of Diagrammatics

To calculate a Fourier-transformed, amputated amplitude, use the following rules:

1. An amputated external line carries the momentum $q_e^{\sigma_e}$; $\sigma_e = +1$ if the line is directed into the future, $\sigma_e = -1$ if it runs into the past:

$$q_e^{\sigma_e} = (\sigma_e \sqrt{\vec{q}^2 + m^2}, \vec{q})^T. \quad (29)$$

2. For a general, non-tadpole vertex write a factor

$$\begin{aligned} \frac{g}{4!} \Psi(-p_1^{\sigma_1}, -p_2^{\sigma_2}, -p_3^{\sigma_3}, -p_4^{\sigma_4}) &= \\ &= \frac{g}{3} \left(\cos\left(\frac{1}{2} p_1^{\sigma_1} \tilde{p}_2^{\sigma_2}\right) \cos\left(\frac{1}{2} p_3^{\sigma_3} \tilde{p}_4^{\sigma_4}\right) \cos\left(\frac{1}{2} (p_1^{\sigma_1} + p_2^{\sigma_2})(\tilde{p}_3^{\sigma_3} + \tilde{p}_4^{\sigma_4})\right) \right. \\ &\quad \left. + (2) \leftrightarrow (3) + (2) \leftrightarrow (4) \right), \end{aligned} \quad (30)$$

where all momenta are oriented outwards from the vertex.

3. For a tadpole vertex (with loop momentum p_1^+), write a factor

$$\begin{aligned} & \frac{g}{4!} \Phi(p_1^+; -p_2^{\sigma_2}, -p_3^{\sigma_3}) = \\ & = \frac{g}{12} \left(3 + e^{ip_1^+ \tilde{p}_2^{\sigma_2}} + e^{ip_1^+ \tilde{p}_3^{\sigma_3}} + e^{ip_1^+ (\tilde{p}_2^{\sigma_2} + \tilde{p}_3^{\sigma_3})} \right) \cos \left(\frac{1}{2} p_2^{\sigma_2} \tilde{p}_3^{\sigma_3} \right), \end{aligned} \quad (31)$$

where p_2, p_3 are oriented outwards from the vertex.

4. For an inner line, write the propagator

$$i\Delta^{TO} = \frac{i}{2\omega} \frac{\delta_{\sigma, -\sigma'}}{\sigma p^0 - \omega_p + i\varepsilon}. \quad (32)$$

5. Sum over all σ 's of the internal lines in order to include all possible contributions with respect to the time ordering of the inner vertices.

6. Integrate over all loop momenta (including tadpole momenta).

Remember that 4-momentum conservation is valid at all vertices and along all lines.

4 Examples for the Application of the Feynman Rules for NC-IPTOPT

In order to both illustrate the applicability and demonstrate the validity of the new-found FR (and since a motivation was given for them, rather than a derivation), we employ them in the recalculation of the diagrams of section 2.

In addition we will finally be able to calculate the “mouse”-diagram $\Gamma^{(2,3)}$, which was one of the main motivations for the development of this diagrammatics.

4.1 The Diagrammatic Tadpole

Once again we turn toward the tadpole, obtained by explicitly commuting out the free-field operators in [9] and by use of the IPTOPT formula eq. (39), *ibidem*.

Simplifying eq. (28) by using 4-momentum conservation $p_2^\mu =: q^\mu = -p_3^\mu$, setting the external momenta on-shell $\sigma_2 = +1, \sigma_3 = -1$, and defining $p_1^+ =: k^+, p_\mu \Theta^{\mu\nu} =: \tilde{p}$ we find for the vertex factor

$$\frac{g}{4!} \Phi(k^+; -q^+, q^+) = \frac{g}{6} (2 + \cos(k^+ \tilde{q}^+)). \quad (33)$$

Note that the σ of the looped line does not occur. Multiplying with the propagator eq. (18), summing over σ, σ' and integrating over phase space

then yields the FT NC tadpole amplitude, which is well known by now:

$$\begin{aligned}
\Gamma^{(2,1)} &= \int \frac{d^4 k}{(2\pi)^4} \frac{g}{6} (2 + \cos(k^+ \tilde{q}^+)) \sum_{\sigma, \sigma'}^{\pm 1} \frac{\delta_{\sigma, -\sigma'}}{2\omega} \frac{i}{\sigma k^0 - \omega_k + i\varepsilon} \\
&= \int \frac{d^4 k}{(2\pi)^4} \frac{g}{6} (2 + \cos(k^+ \tilde{q}^+)) \frac{i}{2\omega_k} \left(\frac{1}{k^0 - \omega_k + i\varepsilon} - \frac{1}{k^0 + \omega_k - i\varepsilon} \right) \\
&= \frac{g}{6} \int \frac{d^3 k}{(2\pi)^3} \frac{1}{2\omega_k} (2 + \cos(k^+ \tilde{q}^+)). \tag{34}
\end{aligned}$$

The actual k^0 -integration can be performed directly for both terms separately, heeding non-vanishing semicircles at infinity. Alternatively they can be brought over a common denominator, resulting in the usual Feynman propagator.

4.2 The Diagrammatic Snowman

To further strengthen our confidence in Δ^{TO} and the vertices of eqs. (27) and (28), we demonstrate how to utilize them to evaluate the snowman of section 2.2.

To obtain the amputated, FT snowman amplitude, we multiply the terms for the two vertices with each other and with one Δ^{TO} for the head-loop and two for the body-loop. Using 4-momentum conservation $k_3^\mu = -k_2^\mu$, $k_3^\pm = -k_2^\mp$, summing over $\sigma_1^v, \sigma_1^w, \sigma_2^v, \sigma_2^w, \sigma_3^v, \sigma_3^w = \pm 1$ and integrating over the two loop-momenta k_1^μ, k_2^μ , we find

$$\begin{aligned}
\Gamma^{(2,2)} &= \frac{g}{4!} \int \frac{d^4 k_1}{(2\pi)^4} \\
&\quad \overbrace{\sum_{\sigma_2^v, \sigma_2^w, \sigma_3^v, \sigma_3^w}^{+, -} \frac{g}{4!} \int \frac{d^4 k_2}{(2\pi)^4} \sum_{\sigma_1, \sigma'_1} \frac{i}{2\omega_1} \frac{\delta_{\sigma_1, -\sigma'_1}}{\sigma_1 k_1^0 - \omega_1 + i\varepsilon} \Phi^v(k_1^+; -k_2^{\sigma_2^v}, +k_2^{-\sigma_3^v})}^{\Gamma^{(2,1)}(k_2; \sigma_2^v, \sigma_3^v)} \\
&\quad \times \Psi^w(-q_e^-, -q_f^+, +k_2^{-\sigma_2^w}, -k_2^{+\sigma_3^w}) \\
&\quad \times \frac{i}{2\omega_2} \frac{i}{2\omega_2} \frac{\delta_{\sigma_2^v, -\sigma_2^w}}{\sigma_2^v k_2^0 - \omega_2 + i\varepsilon} \frac{\delta_{\sigma_3^v, -\sigma_3^w}}{-\sigma_3^v k_2^0 - \omega_2 + i\varepsilon} \\
&= \frac{ig^2}{(4!)^2} \int \frac{d^4 k_1}{(2\pi)^4} \frac{d^4 k_2}{(2\omega_2)^2 (2\pi)^4} \\
&\quad \sum_{\sigma_2^v, \sigma_3^v}^{+, -} \Phi^v(k_1^+; -k_2^{\sigma_2^v}, +k_3^{-\sigma_3^v}) \Psi^w(-q_e^-, -q_f^+, +k_2^{\sigma_2^v}, -k_2^{-\sigma_3^v}) \\
&\quad \times \frac{1}{(k_1^0)^2 - \omega_1^2 + i\varepsilon} \frac{1}{\sigma_2^v k_2^0 - \omega_2 + i\varepsilon} \frac{1}{\sigma_3^v k_2^0 + \omega_2 - i\varepsilon}
\end{aligned}$$

$$\begin{aligned}
&= \frac{g^2}{(4!)^2} \int \frac{d^3 k_1}{2\omega_1(2\pi)^3} \frac{d^3 k_2}{(2\omega_2)^2(2\pi)^3} \frac{dk_2^0}{2\pi} \\
&\quad \left(\Phi^v(k_1^+; -k_2^+, +k_2^-) \Psi^w(-q_e^-, -q_f^+, +k_2^+, -k_2^-) \right. \\
&\quad \times \frac{1}{+k_2^0 - \omega_2 + i\varepsilon} \frac{1}{+k_2^0 + \omega_2 - i\varepsilon} \\
&\quad + \Phi^v(k_1^+; -k_2^+, +k_2^+) \Psi^w(-q_e^-, -q_f^+, +k_2^+, -k_2^+) \\
&\quad \times \frac{1}{+k_2^0 - \omega_2 + i\varepsilon} \frac{1}{-k_2^0 + \omega_2 - i\varepsilon} \\
&\quad + \Phi^v(k_1^+; -k_2^-, +k_2^-) \Psi^w(-q_e^-, -q_f^+, +k_2^-, -k_2^-) \\
&\quad \times \frac{1}{-k_2^0 - \omega_2 + i\varepsilon} \frac{1}{+k_2^0 + \omega_2 - i\varepsilon} \\
&\quad + \Phi^v(k_1^+; -k_2^-, +k_2^+) \Psi^w(-q_e^-, -q_f^+, +k_2^-, -k_2^+) \\
&\quad \left. \times \frac{1}{-k_2^0 - \omega_2 + i\varepsilon} \frac{1}{-k_2^0 + \omega_2 - i\varepsilon} \right). \tag{35}
\end{aligned}$$

In the last step we integrated over k_1^0 as in section 4.1 and expanded the sums over σ_2^v, σ_3^a .

Performing the k_2^0 integration reveals how Δ^{TO} selects the correct σ -signs: the poles in the second and the third term are double poles, both lying on top of each other in the same complex half-plane. Hence we may close the contour in the other half without enclosing any residuum, yielding a vanishing integral (mark that the auxiliary semicircle is harmless, contrary to the tadpole case).

In the first and the fourth term the poles lie in opposite halves and yield upon integration $2\pi i/(2\omega_2)$. Hence we find

$$\begin{aligned}
\Gamma^{(2,2)} &= -\frac{ig^2}{(4!)^2} \int \frac{d^3 k_1}{2\omega_1(2\pi)^3} \frac{d^3 k_2}{(2\omega_2)^3(2\pi)^3} \\
&\quad \left(\Phi(k_1^+; -k_2^+, +k_2^-) \Psi(-q_e^-, -q_f^+, +k_2^+, -k_2^-) + \right. \\
&\quad \left. \Phi(k_1^+; -k_2^-, +k_2^+) \Psi(-q_e^-, -q_f^+, +k_2^-, -k_2^+) \right). \tag{36}
\end{aligned}$$

Evaluation of the phases Φ and Ψ , using momentum conservation $q_e^- = -q_f^+$ and doing some trivial but tedious trigonometry, yields

$$\begin{aligned}
\Phi(k_1^+; -k_2^+, +k_2^-) &= \\
&2 \cos\left(\frac{1}{2}k_2^+ \tilde{k}_2^-\right) (3 + e^{-ik_1^+ \tilde{k}_2^+} + e^{+ik_1^+ \tilde{k}_2^-} + e^{-ik_1^+ (\tilde{k}_2^+ - \tilde{k}_2^-)}) \\
\Phi(k_1^+; -k_2^-, +k_2^+) &= \\
&2 \cos\left(\frac{1}{2}k_2^+ \tilde{k}_2^-\right) (3 + e^{+ik_1^+ \tilde{k}_2^+} + e^{-ik_1^+ \tilde{k}_2^-} + e^{+ik_1^+ (\tilde{k}_2^+ - \tilde{k}_2^-)}) \\
\Psi(-q_e^-, -q_f^+, +k_2^+, -k_2^-) &= 4 \cos\left(\frac{1}{2}k_2^+ \tilde{k}_2^-\right) (3 + \cos(k_2^+ \tilde{q}_f^+) +
\end{aligned}$$

$$\cos(k_2^- \tilde{q}_f^+) + \cos((k_2^+ - k_2^-) \tilde{q}_f^+)) \\ \Psi(-q_e^-, -q_f^+, +k_2^-, -k_2^+) = \Psi(-q_e^-, -q_f^+, -k_2^+, +k_2^-).$$

Inserting this into eq. (36) we find exactly the same result as eq. (11), as obtained by the TO procedure in section 2.2.

4.3 The Diagrammatic Fish

To demonstrate that our diagrammatic rules also work in a non-tadpolie context, we recalculate the t -channel four-point one-loop fish graph evaluated in section 2.3. As above we restrict ourselves to the t -channel.

Using the same notation as in fig. 3, we fix the external on-shell momenta as above: $\sigma_e = -1, \sigma_f = +1, \sigma_g = -1, \sigma_h = +1$. 4-momentum conservation yields

$$\vec{k}_3 = -\vec{k}_2 - \vec{q}_e - \vec{q}_f, \quad k_3^0 = -k_2^0 + \omega_e - \omega_f. \quad (37)$$

$\Gamma^{(4,1)}$ is then given as

$$\begin{aligned} \Gamma^{(4,1)} &= \frac{g^2}{(4!)^2} \int \frac{d^4 k_2}{(2\pi)^4} \sum_{\sigma_2^w, \sigma_2^v, \sigma_3^w, \sigma_3^v}^{+1, -1} \frac{i}{2\omega_2} \frac{i}{2\omega_3} \\ &\quad \Psi^w(-q_e^-, -q_f^+, -k_2^{\sigma_2^w}, -k_3^{\sigma_3^w}) \Psi^v(-q_g^-, -q_h^+, +k_2^{-\sigma_2^v}, +k_3^{-\sigma_3^v}) \\ &\quad \frac{\delta_{\sigma_2^w, -\sigma_2^v}}{\sigma_2^w k_2^0 - \omega_2 + i\varepsilon} \frac{\delta_{\sigma_3^w, -\sigma_3^v}}{-\sigma_3^w (k_2^0 + \omega_e - \omega_f) - \omega_3 + i\varepsilon} \\ &= \frac{g^2}{(4!)^2} \int \frac{d^4 k_2}{(2\pi)^4} \sum_{\sigma_2^w, \sigma_3^w}^{+1, -1} \frac{1}{2\omega_2 2\omega_3} \\ &\quad \Psi^w(-q_e^-, -q_f^+, -k_2^{\sigma_2^w}, -k_3^{\sigma_3^w}) \Psi^v(-q_g^-, -q_h^+, +k_2^{+\sigma_2^w}, +k_3^{+\sigma_3^w}) \\ &\quad \frac{1}{\sigma_2^w k_2^0 - \omega_2 + i\varepsilon} \frac{1}{\sigma_3^w k_2^0 + \sigma_3^w \omega_e - \sigma_3^w \omega_f + \omega_3 - i\varepsilon} \\ &= \frac{g^2}{(4!)^2} \int \frac{d^4 k_2}{(2\pi)^4} \frac{1}{2\omega_2} \frac{1}{2\omega_3} \\ &\quad \left(\frac{\Psi^w(-q_e^-, -q_f^+, -k_2^+, -k_3^+)}{k_2^0 - \omega_2 + i\varepsilon} \frac{\Psi^v(-q_g^-, -q_h^+, +k_2^+, +k_3^+)}{k_2^0 + \omega_e - \omega_f + \omega_3 - i\varepsilon} \right. \\ &\quad + \frac{\Psi^w(-q_e^-, -q_e^+, -k_2^+, -k_3^-)}{+k_2^0 - \omega_2 + i\varepsilon} \frac{\Psi^v(-q_g^-, -q_h^+, +k_2^+, +k_3^-)}{-k_2^0 - \omega_e + \omega_f + \omega_3 - i\varepsilon} \\ &\quad + \frac{\Psi^w(-q_e^-, -q_f^+, -k_2^-, -k_3^+)}{-k_2^0 - \omega_2 + i\varepsilon} \frac{\Psi^v(-q_g^-, -q_h^+, +k_2^-, +k_3^+)}{+k_2^0 + \omega_e - \omega_f + \omega_3 - i\varepsilon} \\ &\quad \left. + \frac{\Psi^w(-q_e^-, -q_f^+, -k_2^-, -k_3^-)}{-k_2^0 - \omega_2 + i\varepsilon} \frac{\Psi^v(-q_g^-, -q_h^+, +k_2^-, +k_3^-)}{-k_2^0 - \omega_e + \omega_f + \omega_3 - i\varepsilon} \right). \quad (38) \end{aligned}$$

Inspecting the complex k_2^0 plane of the four terms we see that the poles of the second and the third term lie on the same half-plane and hence yield

vanishing integrals. We thus find (for shortness we retain k_3, ω_3 , but of course eqs. (37) still apply)

$$\begin{aligned} \Gamma^{(4,1)} = & \frac{-ig^2}{(4!)^2} \int \frac{d^3 k_2}{(2\pi)^3} \frac{1}{2\omega_2} \frac{1}{2\omega_3} \\ & \left(\frac{\Psi^w(-q_e^-, -q_f^+, -k_2^+, -k_3^+) \Psi^v(-q_g^-, -q_h^+, +k_2^+, +k_3^+)}{\omega_2 + \omega_3 + \omega_e - \omega_f - i\varepsilon} \right. \\ & \left. + \frac{\Psi^w(-q_e^-, -q_f^+, -k_2^-, -k_3^-) \Psi^v(-q_g^-, -q_h^+, +k_2^-, +k_3^-)}{\omega_2 + \omega_3 - (\omega_e - \omega_f) - i\varepsilon} \right), \end{aligned} \quad (39)$$

which is identical to eq. (13).

4.4 The Diagrammatic Mouse - where the UV/IR Mixing should occur

Confident in our new tools, we embark on calculating the two-point three-loop amplitude of “mouse-like morphology”, figure 4.

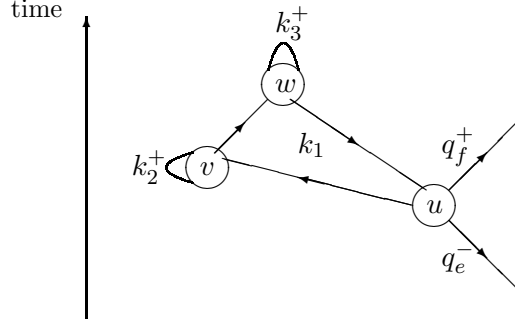


Figure 4: The macro-contribution uvw

This amplitude is of great interest since in usual non-commutative QFT it is the simplest graph that becomes undefined due to the notorious UV/IR-mixing problem: the two tadpoles inserted into the third each bring a $1/\tilde{k}_1^2$, introducing a non-integrable IR-singularity into the remaining, otherwise UV-finite, loop-integral – usually...

Beginning as in the previous sections (and skipping the steps that are now familiar), the amplitude of interest is written as

$$\begin{aligned} \Gamma^{(2,3)} = & \\ & \frac{ig^3}{(4!)^3} \int \frac{d^4 k_1}{(2\pi)^4} \frac{d^4 k_2}{(2\pi)^4} \frac{d^4 k_3}{(2\pi)^4} \frac{1}{(2\omega_1)^3} \frac{1}{2\omega_2} \frac{1}{2\omega_3} \end{aligned}$$

$$\begin{aligned}
& \sum_{\sigma_2, \sigma_3}^{+1, -1} \frac{1}{\sigma_2 k_2^0 - \omega_2 + i\varepsilon} \frac{1}{\sigma_3 k_3^0 - \omega_3 + i\varepsilon} \\
& \sum_{\sigma_u, \sigma_v, \sigma_w}^{+1, -1} \Phi^v(k_2^+; k_1^{\sigma_u}, -k_1^{\sigma_v}) \Phi^w(k_3^+; k_1^{\sigma_v}, -k_1^{\sigma_w}) \Psi^u(q_f^+, -q_f^+, k_1^{\sigma_w}, -k_1^{\sigma_u}) \\
& \frac{1}{\sigma_u k_1^0 - \omega_1 + i\varepsilon} \frac{1}{\sigma_v k_1^0 - \omega_1 + i\varepsilon} \frac{1}{\sigma_w k_1^0 - \omega_1 + i\varepsilon}. \tag{40}
\end{aligned}$$

Two of the eight possible combinations of $\sigma_u = \pm, \sigma_v = \pm, \sigma_w = \pm$ result in the coincidence of all three poles on the same half of the complex plane, and they thus vanish under k_1^0 -integration. The remaining six summands yield

$$\begin{aligned}
& \Gamma^{(2,3)} = \\
& \frac{ig^3}{(4!)^3} \left(-i \int \frac{d^3 k_1}{(2\pi)^3} \frac{1}{(2\omega_1)^5} \right) \left(-i \int \frac{d^3 k_2}{(2\pi)^3} \frac{1}{2\omega_2} \right) \left(-i \int \frac{d^3 k_3}{(2\pi)^3} \frac{1}{2\omega_3} \right) \\
& \left(\Phi^v(k_2^+; k_1^+, -k_1^+) \Phi^w(k_3^+, k_1^+, -k_1^-) \Psi^u(q_f^+, -q_f^+, k_1^-, -k_1^+) \right. \\
& + \Phi^v(k_2^+; k_1^+, -k_1^-) \Phi^w(k_3^+, k_1^-, -k_1^+) \Psi^u(q_f^+, -q_f^+, k_1^+, -k_1^+) \\
& + \Phi^v(k_2^+; k_1^-, -k_1^+) \Phi^w(k_3^+, k_1^+, -k_1^+) \Psi^u(q_f^+, -q_f^+, k_1^+, -k_1^-) \\
& + \Phi^v(k_2^+; k_1^+, -k_1^-) \Phi^w(k_3^+, k_1^-, -k_1^-) \Psi^u(q_f^+, -q_f^+, k_1^-, -k_1^+) \\
& + \Phi^v(k_2^+; k_1^-, -k_1^+) \Phi^w(k_3^+, k_1^+, -k_1^-) \Psi^u(q_f^+, -q_f^+, k_1^-, -k_1^-) \\
& \left. + \Phi^v(k_2^+; k_1^-, -k_1^-) \Phi^w(k_3^+, k_1^-, -k_1^+) \Psi^u(q_f^+, -q_f^+, k_1^+, -k_1^-) \right). \tag{41}
\end{aligned}$$

Here the six terms correspond to the six possible macro-time orderings of the vertices: $uvw, wuv, vwu, uwv, vuw, wvu$, respectively.

5 No UV/IR Mixing in IPTOPT

The most interesting feature of IPTOPT is the apparent absence of the UV/IR-mixing problem. This can be seen in the amplitudes calculated so far by explicitly performing the loop integrations in the result of the previous section 4.4. No divergence will be fed down via the phases to the next loop.

5.1 Explicit Result for the UV/IR Divergence-free Mouse

To evaluate eq. (41) explicitly, we start by integrating over k_2 and k_3 . These integrals yield, apart from a possible overall cosine in k_1 , exactly the \mathcal{I} 's from

section 3.1 and [9]:

$$\begin{aligned}
& \int \frac{d^3 k}{(2\pi)^3} \frac{1}{2\omega} \Phi(k^+; k_1^\sigma, -k_1^{\sigma'}) \\
&= \int \frac{d^3 k}{(2\pi)^3} \frac{2}{2\omega} \cos\left(\frac{1}{2} k_1^\sigma \tilde{k}_1^{\sigma'}\right) \left(3 + e^{-ik^+ \tilde{k}_1^\sigma} + e^{ik^+ \tilde{k}_1^{\sigma'}} + e^{-ik^+ (\tilde{k}_1^\sigma - \tilde{k}_1^{\sigma'})}\right) \\
&= 2 \cos\left(\frac{1}{2} k_1^\sigma \tilde{k}_1^{\sigma'}\right) \mathcal{I}(k_1^\sigma, -k_1^{\sigma'}).
\end{aligned} \tag{42}$$

Since these were already evaluated in eq. (20)–(26), determining the result for all but the last loop integration is a mere task of compilation. Using the same abbreviations as above ($k_1 \rightarrow k$) we find

$$\begin{aligned}
& \Gamma^{(2,3)} = \\
& -\frac{g^3}{4(3!)^3 (2\pi)^4} \int \frac{d^3 k}{(2\pi)^3} \frac{1}{(2\omega)^5} \left[1 + \cos(k^+ \tilde{k}^-) \right] \\
& \times \left[\frac{3}{2} \mathcal{Q} - \frac{2m}{|\tilde{k}^+|} K_1(m|\tilde{k}^+|) - \frac{2m}{|\tilde{k}^-|} K_1(m|\tilde{k}^-|) + \frac{m}{\omega_k |\Theta_{0i}|} K_1(2m\omega_k |\Theta_{0i}|) \right] \\
& \times \left[\left(4 + \cos(k^+ \tilde{q}_f^+) + \cos(k^- \tilde{q}_f^+) \right) \right. \\
& \times \left(\frac{3}{2} \mathcal{Q} - \frac{2m}{|\tilde{k}^+|} K_1(m|\tilde{k}^+|) - \frac{2m}{|\tilde{k}^-|} K_1(m|\tilde{k}^-|) + \frac{m}{\omega_k |\Theta_{0i}|} K_1(2m\omega_k |\Theta_{0i}|) \right) \\
& + \left. \left(3 + \cos(k^+ \tilde{q}_f^+) + \cos(k^- \tilde{q}_f^+) + \cos((k^+ - k^-) \tilde{q}_f^+) \right) \right. \\
& \times \left. \left(2\mathcal{Q} - \frac{m}{|\tilde{k}^+|} K_1(m|\tilde{k}^+|) - \frac{m}{|\tilde{k}^-|} K_1(m|\tilde{k}^-|) \right) \right]
\end{aligned} \tag{43}$$

where $K_1(x)$ is the modified Bessel function. So far in non-commutative QFT this expression contained an IR divergence: poles in k^2 of 2nd order. This is not the case here as

$$\lim_{\tilde{k} \rightarrow 0} (\tilde{k}_\mu^\pm)^2 = -m^2 \Theta_{0i}^2 < 0. \tag{44}$$

This limit will be discussed in more detail in the next section.

Where does this first instance of the absence of the notorious UV/IR-mixing problem stem from? It is due to the appearance of on-shell 4-momenta in the non-commutative phases: since, because of the mass, the 0-component remains non-vanishing for all values of the three-momentum, no pole can appear.

5.2 Argument for the General Absence of UV/IR Mixing

Encouraged by the above explicit result we give an argument for the absence of this problem to all orders — for all $\Gamma^{(n,l)}$ — in (IPTO) perturbation theory in a more general way (although we refrain from writing “proof”).

To arrive at this conclusion we remember the n -th order k -point Green functions given by the Gell-Mann–Low formula

$$\begin{aligned} G_n(x_1, \dots, x_k) \\ = \frac{i^n}{n!} \int d^4 z_1 \dots d^4 z_n \langle 0 | T \phi(x_1) \dots \phi(x_k) \mathcal{L}_I(z_1) \dots \mathcal{L}_I(z_n) | 0 \rangle^{con}, \end{aligned} \quad (45)$$

where T denotes the time ordering and $\mathcal{L}_I(z)$ is the interaction part of the Lagrangian, $\frac{g}{4!}(\phi \star \phi \star \phi \star \phi)$ for non-commutative ϕ^4 -theory.

Note that all fields occurring in eq. (45) are *free fields*, their Fourier transforms are on-shell quantities, the 0-component of the four-vector being $\omega(\vec{k})$:

$$\phi(x) = \int \frac{d^3 k}{(2\pi)^3} \left(\tilde{\phi}(\vec{k}) e^{-ik^+ x} + \tilde{\phi}^\dagger(\vec{k}) e^{+ik^+ x} \right). \quad (46)$$

Evaluating the \star -product between these FT free fields hence produces phase factors containing *on-shell* momenta k_μ^\pm only (see also the discussion in chapter 3 of [9]). This remains true after integrating out some (or all) of the loop-momenta occurring later in the evaluation. At no point of the further calculations (evaluating TO, FT, amputation, ...) will this property be changed.

Why does this novel feature of IPTOPT prohibit the occurrence of the usual UV/IR problem? First note that for timelike (on-shell) four vectors k^μ we find \tilde{k}^μ to be spacelike

$$\Theta_{\mu\nu} k^\mu k^\nu = 0 = (k^\mu (\Theta_{\mu\nu}) k^\nu) := \tilde{k}^\mu k_\mu \quad (47)$$

and hence

$$\tilde{k}^\mu \tilde{k}_\mu < 0 \quad \forall \tilde{k}^\mu \neq 0^\mu \quad , \quad \tilde{k}^\mu \tilde{k}_\mu = 0 \leftrightarrow \tilde{k}^\mu = 0^\mu. \quad (48)$$

The case $\tilde{k}^\mu = 0^\mu$ is only possible for massive theories iff $\Theta_{\mu\nu}$ is of less than full rank, which is excluded in IPTOPT since we demand $\Theta_{i0} \neq 0$: if $\Theta_{\mu\nu}$ were of less than full rank, one could always transform it into $\Theta'_{\mu\nu}$, with $\Theta'_{i0} = 0$, which we excluded by definition.

Hence we find

$$\tilde{k}^2 = \tilde{k}^\mu \tilde{k}_\mu < 0 \quad \forall \tilde{k}. \quad (49)$$

As the usual (i.e. the one found in the literature) UV/IR problem always occurs in the form of a $1/\tilde{k}^2$ pole, which, for off-shell k^μ and \tilde{k}^μ , introduces a possible new singularity at 0, we see that IPTOPT is free from this (type of) problem: zero is never reached by \tilde{k}^2 .

It is at this point that our argument degrades from being a proof, since it excludes the appearance of this particular form of mixing only. But in what other guises it still has to be excluded we are not able to discuss yet.

5.3 A short Note on PT

As a short side-remark we would like to draw your attention to the behaviour of the amplitudes calculated above under P and/or T acting on the external momenta:

$$P : \vec{q} \rightarrow -\vec{q}, \quad T : \sigma \rightarrow -\sigma. \quad (50)$$

Hence we find that

$$P(q^\pm) = -q^\mp, \quad T(q^\pm) = q^\mp, \quad (51)$$

which do not leave the amplitudes calculated above invariant when only one of P, T acts on them. However, under the combined action of PT :

$$PT(q^\pm) = P(q^\mp) = -q^\pm, \quad (52)$$

the amplitudes remain unchanged, since the external momenta occur in cosine only.

Invariance under PT , however, is a direct consequence of the unitarity of the S-matrix and the existence of free states; see [14] and references therein.

6 Outlook

In this article one further step was taken in the program of IPTOPT: Feynman rules were stated and demonstrated to yield the same results as the TO amplitude. In a sense, IPTOPT developed into interaction-point diagrammatics. Although note must be taken that these FR are rather conjectured than truly derived, since (Minkowskian) canonical instead of (Euclidean) PI quantization was employed. A more general and rigorous method for obtaining them has recently been found in [12].

Also a strong motivation for further work utilizing this approach was discovered: the possibility of the general absence of the UV/IR problem. Although a strong argument in favour of this feature was given, a true proof is still missing and certainly highly desirable. In principle two routes to this end are imaginable: either continuing in IPTOPT, investigating eq. (2) for the possibility of an inductive proof; or by making use of the diagrammatics proposed in this work. The second approach could also yield important insights into how to pursue the great question of renormalizability and renormalization of non-commutative QFT.

Further work may deepen our understanding of the intricate connections between nano-causality, unitarity, UV/IR mixing (i.e. its absence), CPT invariance and renormalization. Moreover, possible phenomenological implications of IPTOPT will be of great interest [15]. Anyway, with non-commutative QFT a tool to a better understanding of commutative QFT is available, illustrating by similarities and differences the fundamental features of the two sets of theories.

Acknowledgements

VP would like to thank Prof. M. Schweda and R. Wulkenhaar for helpful discussion and support. PF would like to thank C. Jarlskog, T. Hurth, L. Álvarez-Gaumé and A. Bichl for lectorship and discussions, S. Vascotto for excellent and thorough linguistic corrections.

References

- [1] S. Minwalla, M. Van Raamsdonk and N. Seiberg, “Noncommutative perturbative dynamics,” *JHEP* **0002** (2000) 020 [arXiv:hep-th/9912072].
- [2] A. Matusis, L. Susskind and N. Toumbas, “The IR/UV connection in the non-commutative gauge theories,” *JHEP* **0012** (2000) 002 [arXiv:hep-th/0002075].
- [3] D. Bahns, S. Doplicher, K. Fredenhagen and G. Piacitelli, “On the unitarity problem in space/time non-commutative theories,” *Phys. Lett. B* **533** (2002) 178 [arXiv:hep-th/0201222].
- [4] J. Gomis and T. Mehen, “Space-time non-commutative field theories and unitarity,” *Nucl. Phys. B* **591** (2000) 265 [arXiv:hep-th/0005129].
- [5] S. Doplicher, K. Fredenhagen and J. E. Roberts, “The quantum structure of space-time at the Planck scale and quantum fields,” *Commun. Math. Phys.* **172** (1995) 187 [arXiv:hep-th/0303037].
- [6] C. H. Rim and J. H. Yee, “Unitarity in space-time noncommutative field theories,” [arXiv:hep-th/0205193].
- [7] Y. Liao and K. Sibold, “Time-ordered perturbation theory on non-commutative spacetime: Basic rules,” *Eur. Phys. J. C* **25** (2002) 469 [arXiv:hep-th/0205269].
- [8] Y. Liao and K. Sibold, “Time-ordered perturbation theory on non-commutative spacetime. II. Unitarity,” *Eur. Phys. J. C* **25** (2002) 479 [arXiv:hep-th/0206011].
- [9] H. Bozkaya, P. Fischer, H. Grosse, M. Pitschmann, V. Putz, M. Schweda, R. Wulkenhaar, “Space/time noncommutative field theories and causality,” *Eur. Phys. J. C* **29** (2003) 133 [arXiv:hep-th/0209253].
- [10] D. Bahns, S. Doplicher, K. Fredenhagen and G. Piacitelli, “Ultraviolet finite quantum field theory on quantum spacetime,” *Commun. Math. Phys.* **237** (2003) 221 [arXiv:hep-th/0301100].

- [11] See e.g. eq. (9.72) of G. Sterman, “An Introduction to Quantum Field Theory,” Cambridge Univ. Press, 1993.
- [12] S. Denk and M. Schweda, “Time ordered perturbation theory for non-local interactions; applications to NCQFT,” TUW-03-19 [arXiv:hep-th/0306101]
- [13] A. Miku and M. M. Sheik-Jabbari, “Non-commutative ϕ^4 theory at two loops,” JHEP **0101** (2001) 025, [arXiv:hep-th/0008057].
- [14] L. Álvarez-Gaumé and M. A. Vázquez-Mozo, “General properties of non-commutative field theories,” CERN-TH/2003-100, HU-EP-03/19, [arXiv:hep-th/0305093].
- [15] Y. Liao and C. Dehne, “Some phenomenological consequences of the time-ordered perturbation theory of QED on non-commutative space-time,” [arXiv:hep-ph/0211425].